Acta Materia Medica

Research Article

# Identification of GPR35-associated metabolic characteristics through LC-MS/MS-based metabolomics and lipidomics

## Graphical abstract

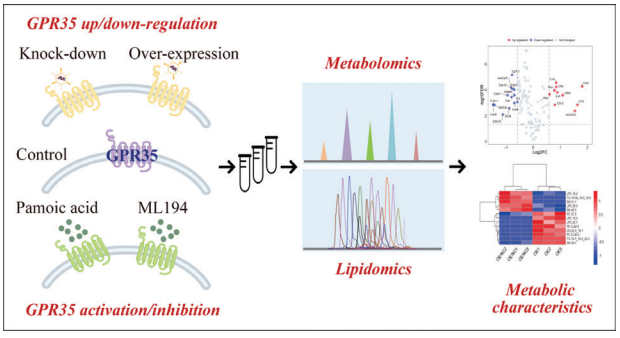


## Highlights

- Four G protein-coupled receptor 35 (GPR35) intervention cell models exhibit significant alterations in the levels of 75 metabolites and 204 lipids.
- The metabolites 3-hydroxyanthranilic acid (HAA) and uracil (Ura) demonstrate sensitivity across all GPR35 interventions.
- GPR35 interventions notably disturb fatty acid β-oxidation and phosphatidylethanolamine metabolism pathways.

## Authors

Qiqing Zhang, Xian Zhao, Siyuan Qin, Qinwen Xiao, Yuan Tian, Zunjian Zhang, Pei Zhang and Fengguo Xu

## Correspondence

fengguoxu@cpu.edu.cn, Fax/Tel: +86-025-83271021 (F. Xu); peizhangcpu@cpu.edu.cn, Fax/Tel: +86-025-83271021 (P. Zhang)

## In brief

G protein-coupled receptor 35 (GPR35) interventions had a significant impact on the abundance of downstream metabolites and lipids, particularly affecting those involved in β-oxidation and phosphatidylethanolamine pathways.

https://doi.org/10.15212/AMM-2023-0046
Acta Materia Medica 2024, Volume 3, Issue 1, p. 105-118 

Acta Materia Medica

Research Article

# Identification of GPR35-associated metabolic characteristics through LC-MS/MS-based metabolomics and lipidomics

**Qiqing Zhang[a], Xian Zhao[b,c], Siyuan Qin[a], Qinwen Xiao[a], Yuan Tian[a], Zunjian Zhang[a], Pei Zhang[a,*] and Fengguo Xu[a,d,*]**

[a]Key Laboratory of Drug Quality Control and Pharmacovigilance (Ministry of Education), China Pharmaceutical University, Nanjing 210009, P. R. China
[b]Department of Pharmacy, China Pharmaceutical University Nanjing Drum Tower Hospital, Nanjing 210008, P. R. China
[c]Department of Pharmacy, Nanjing Drum Tower Hospital, Affiliated Hospital of Medical School, Nanjing University, Nanjing 210008, P. R. China
[d]School of Traditional Chinese Pharmacy, China Pharmaceutical University, Nanjing 210009, P. R. China

***Correspondence:** fengguoxu@cpu.edu.cn, Fax/Tel: +86-025-83271021 (F. Xu); peizhangcpu@cpu.edu.cn, Fax/Tel: +86-025-83271021 (P. Zhang)

Received: 5 December 2023; Revised: 23 February 2024; Accepted: 6 March 2024

Published online: 26 March 2024

DOI 10.15212/AMM-2023-0046

## ABSTRACT

G protein-coupled receptor 35 (GPR35) has gained increasing attention as a promising target in treating inflammatory and gastrointestinal tract conditions, cardiovascular diseases, and cancer. Metabolites including kynurenic acid, lysophosphatidic acids, chemokine 17, and 5-hydroxyindole acetic acid have been suggested to be endogenous ligands of GPR35. However, little is known regarding the downstream metabolic characteristics upon GPR35 regulation. Herein, four GPR35 interventions in cell models, comprising GPR35 knock-down, over-expression, activation, or inhibition, were established through lentiviral transduction, or the use of a potent agonist (pamoic acid) or antagonist (ML194). Targeted metabolomics and pseudotargeted lipidomics were performed on these cell models to capture GPR35-associated metabolites and lipids. Levels of 75 metabolites and 204 lipids were significantly altered in response to one or more GPR35 interventions. Levels of metabolites involved in fatty acid β-oxidation and phosphatidylethanolamine metabolism were notably altered. This study reports the first exploration of the metabolic characteristics of GPR35, and may aid in understanding of the potential mechanisms and functions of GPR35 in various physiological and pathological conditions.

**Keywords:** GPR35, metabolomics, lipidomics, FAO, PE metabolism

## 1. INTRODUCTION

More than one-third of drugs are believed to target G protein-coupled receptors (GPCRs) [1]. However, the ligands and functions of many GPCRs are not well understood; G protein-coupled receptor 35 (GPR35) is one such "orphan" receptor [2]. The GPR35 gene is located on chromosome 2q37.3 in human [2] and produces two variants (GPR35a and b) [3]. This gene is highly expressed in the gastrointestinal tract and immune system, and is moderately expressed in the whole brain, skeletal muscle, liver, and heart [4]. GPR35 has gained increasing attention as a crucial target, owing to its broad pathophysiological association with many diseases. GPR35 plays a substantial role in intestinal homeostasis [4]. $GPR35^{-/-}$ mice treated with dextran sulfate sodium show more severe colitis syndrome than wild-type mice [5]. Activation of the GPR35 pathway promotes colorectal tumor growth [6, 7]. Furthermore, GPR35 has been reported to act in various subpopulations of immune cells; e.g., activated GPR35 decreases interleukin-4 secretion in invariant natural killer T cells [8], promotes neutrophil recruitment [9], and induces cell-cycle arrest in monocytes [10]. GPR35 is also associated with cardiovascular diseases. Genome-wide association studies have indicated that GPR35 is significantly up-regulated in patients with heart failure [11]. Activation of GPR35 protects against ischemia during myocardial infarction [12], and $GPR35^{-/-}$ relieves angiotensin II-induced hypertension [13]. In addition,

Acta Materia Medica

GPR35 has been implicated in pain perception [14], cancer [15], and type 2 diabetes [16].

GPR35 activates $G_s$, $G_i$, $G_q$, and $G_{12/13}$, and regulates other signaling pathways through second messengers (e.g., cyclic adenosine monophosphate, $Ca^{2+}$, and diacylglycerol), thereby exerting physiological functions [4]. GPR35 alleviates ulcerative colitis (UC) through complementary mechanisms; i.e., GPR35 inhibits NOD-like receptor thermal protein domain associated protein 3 over-activation and thus relieves inflammation by reducing the level of interleukin-1β [17], GPR35 also increases the expression of fibronectin and integrin-α5β1, thus promoting the repair of colon mucosa [18]. Furthermore, GPR35 promotes lipid metabolism through various mechanisms. Agudelo et al. [19] have reported that GPR35 increases levels of peroxisome proliferator-activated receptor γ coactivator-1α (PGC-1α) and regulator of G-protein signaling 14, thereby stimulating lipid metabolism and anti-inflammatory gene expression in adipose tissue. In contrast, Nam et al. reported that GPR35 inhibits liver X receptor (LXR), thereby reducing lipid accumulation through the p38 mitogen-activated protein kinase and c-Jun N-terminal kinase pathways in hepatocytes [20]. In addition, GPR35 activates Ras homolog gene family member A/Rho-associated coiled-coil kinase signaling and consequently plays a role in multiple cardiovascular diseases [21, 22]; interacts with $Na^+/K^+$-ATPase and consequently promotes colorectal cancer [6, 7]; and recruits β-arrestin-2 [23, 24], which acts as a scaffold in signal transduction and is associated with receptor desensitization, and the c-Jun, protein kinase B and extracellular-regulated kinase 1/2 (ERK1/2) pathways [25].

GPR35 is strongly associated with metabolic regulation in various physiological and pathological conditions. GPR35 is a member of the metabolite-sensing GPCRs, which bind various metabolites and transmit signals important for proper immune and metabolic functions [26]. Furthermore, GPR35 may act as an integration node in conditions in which inflammation skews metabolism, given that it is expressed in adipose tissue, immune cells, and the gastrointestinal tract, and that metabolic disorders often coincide with states of chronic inflammation [27]. Moreover, activation of GPR35 promotes lipid metabolism in skeletal muscle [28], adipose tissue [19], and liver cells [20, 29]. However, little is known regarding the downstream metabolic characteristics upon GPR35 regulation. Identification of GPR35-associated metabolic characteristics would increase understanding of the potential mechanisms and functions of GPR35 in various physiological and pathological conditions.

## 2. MATERIALS AND METHODS

### 2.1 Chemicals and reagents

Pamoic acid (CAS#130-85-8) and ML194 (CAS#264233-05-8) were purchased from Sigma-Aldrich. Dulbecco's modified eagle medium (DMEM) and fetal bovine serum were obtained from Gibco (Grand Island, NY, United States). Penicillin-streptomycin was obtained from Boster (Wuhan, China). Metabolite standards were purchased from Sigma-Aldrich (St. Louis, MO, USA), Aladdin (Shanghai, China), and J&K Chemical Technology (Beijing, China); 1-[bis (dimethylamino) methylene]-1H-1,2,3-triazolo[4,5-b] pyridinium 3-oxid hexafluorophosphate and 5-dimethylamino-naphthalene-1-sulfonyl chloride (Dns-Cl) were obtained from J&K Chemical Technology; and 5-dimethylamino-naphthalene-1-sulfonyl piperazine (Dns-PP) was synthesized in house, as reported previously [30]. $D_6$-Dns-Cl and $D_6$-Dns-PP were purchased from Wuxi Beita Pharmatech. Liquid chromatography–mass spectrometry (LC–MS) grade reagents, including methanol (MeOH), acetonitrile (ACN), isopropanol (IPA), and methyl tert-butyl ether (MTBE), were obtained from Merck (Darmstadt, Germany). Formic acid was obtained from Nanjing Chemical Reagent (Nanjing, China). Deionized water was produced with a Milli-Q system (Millipore, Massachusetts, United States).

### 2.2 Cell culture

The HCT116 cell line was obtained from Cobioer Biosciences (Nanjing, China), and was cultured in DMEM supplemented with 10% fetal bovine serum and 0.1% penicillin-streptomycin. Cells were cultured at 37°C in a humidified atmosphere containing 5% $CO_2$. The HCT116 cell line was authenticated at Zhong Qiao Xin Zhou Biotechnology (Shanghai, China), with sample code 20170713-06.

### 2.3 Cell transfection

Lentivirus for gene silencing and over-expression of human GPR35 were purchased from GenePharma (Shanghai, China). The lentiviral vector system contained green fluorescent protein and puromycin resistance genes. Cells at 40%–60% confluence were transduced with lentivirus at a multiplicity of infection of 10, and incubated with medium containing 5 μg/mL polybrene (GenePharma, Shanghai). After 24 h, the medium was replaced with fresh culture medium. After 72 h, cells positive for green fluorescent protein were observed under a fluorescence microscope (Nikon, Tokyo, Japan), then selected with medium containing 2 μg/mL puromycin for another 48 h. The oligonucleotide sequences of the lentiviral vectors are listed in **Table S1**.

### 2.4 Analysis of GPR35 internalization

The quantification of receptor internalization was performed by measurement of specific-antibody-tagged receptors on cell surfaces through flow cytometry. Cells were exposed to drugs or vehicles for 48 h, then collected by centrifugation (1,000 rpm, 5 min) (Eppendorf, Hamburg, Germany). Subsequently, cells in the treatment groups were incubated with anti-GPR35 (1:300, Proteintech, Chicago, IL, USA), whereas cells in the

negative control group were incubated with 3% bovine serum albumin in phosphate-buffered saline (PBS) buffer at 4°C for 2 h. All groups were subsequently incubated with secondary antibody Alexa Fluor® 488 conjugate anti-rabbit IgG (H+L) (1:300, Cell Signaling Technology, Boston, MA, USA) at 4°C for 1 h. The cells were then fixed with 4% formaldehyde. The fluorescence intensity of 1 × $10^4$ cells per sample was measured with a NovoCyte system (Agilent, California, United States). The percentage of internalized receptors was calculated from surface receptor fluorescence values (F) according to the following equation:

$$\text{Receptor internalization rate (\%)} = 100 \times \left(F_{\text{Control group}} - F_{\text{Treatment group}}\right) / \left(F_{\text{Control group}} - F_{\text{Negative group}}\right).$$

## 2.5 mRNA preparation and reverse transcription polymerase chain reaction

GPR35 and glyceraldehyde 3-phosphate dehydrogenase (GAPDH) expression was analyzed with a standard reverse transcription polymerase chain reaction (RT-PCR) protocol. Total RNA was extracted from cells with an RNAiso Plus Kit (Takara Biotechnology, Dalian, China). RNA concentrations were detected with a Nano-Drop 2000 instrument (Thermo Fisher Scientific, Waltham, MA, USA). Subsequently, RNA (1 μg) was reverse transcribed to complementary DNA with a PrimeScript™ RT reagent kit (Takara Biotechnology). RT-PCR was performed with SYBR Green I Master Mix (Roche, Basel, Switzerland) on a LightCycler 480 instrument (Roche). The relative expression levels of GPR35 were calculated with the $2^{-\Delta\Delta CT}$ method, on the basis of normalization to GAPDH. The primer sequences for RT-PCR are listed in **Table S2**.

## 2.6 Western blotting analysis

The protein expression of GPR35, ERK1/2, phospho-ERK1/2 (pERK1/2), and α-tubulin was analyzed with a standard western blotting protocol. Cells were lysed with radioimmunoprecipitation assay buffer (Beyotime Biotechnology, Shanghai, China) containing 0.1% phenylmethylsulfonyl fluoride (Thermo Fisher Scientific) on ice, and total protein was extracted. Protein concentrations were measured with a bicinchoninic acid protein assay kit (Beyotime Biotechnology). The lysates were mixed with sample loading buffer (Beyotime Biotechnology) and denatured at 95°C. Protein samples (30 μg) were separated by sodium dodecyl sulfate–polyacrylamide gel electrophoresis with 8% acrylamide gels and transferred to polyvinylidene difluoride membranes (Massachusetts, United States) (0.2 μm) with an electroblotting apparatus (Tanon, Shanghai, China). The membranes were blocked with 5% (w/v) nonfat milk for 2 h at room temperature and incubated with primary antibodies at 4°C overnight. After the membranes were washed three times with PBS containing 0.1% Tween 20, the immunoreactive bands were incubated with secondary antibodies conjugated to horseradish peroxidase for 2 h at room temperature. The immunoreactive bands were subsequently visualized with enhanced chemiluminescence (Massachusetts) with a Tanon 5200 chemiluminescence imaging system (Tanon, Shanghai, China). Relative protein expression was calculated through densitometric analysis in ImageJ software. The antibodies used for western blotting analysis are listed in **Table S3**.

## 2.7 Targeted metabolomic analysis

***2.7.1 Sample preparation.*** A total of ~$10^7$ cells were collected and quenched with 3 mL cold MeOH/$H_2O$ (80/20, v/v) at –80°C for 30 min, then transferred to tubes. Cell suspensions were vortex mixed and ultrasonicated at 100 W for 5 min on ice. The supernatant was collected after centrifugation (12,000 rpm, 10 min, 4°C). Quality control (QC) samples were prepared by pooling equal aliquots of each sample. All samples were evaporated to dryness at 37°C under nitrogen gas for further derivatization. Metabolites containing an amino/phenol group were labeled by Dns-Cl, and the carboxyl group was labeled by Dns-PP (detailed classification information in **Table S4**). The chemical derivatization procedure (Dns-Cl and Dns-PP labeling) was as reported in our previous study [31] and is described in the Extended Methods section in the Supporting Information. A Shimadzu Nexera UPLC system interfaced with an 8060 triple quadruple mass spectrometer (Shimadzu, Kyoto, Japan) was used for metabolomics analysis. Details regarding instrument conditions, columns, mobile phases, and MS parameters can be found in the Extended Methods section of the Supplementary Information. Another aliquot of cells was prepared for total protein assays (Beyotime Biotechnology), and the results were used for metabolite normalization.

## 2.8 Pseudotargeted lipidomics analysis

***2.8.1 Sample preparation.*** A total of ~$10^7$ cells were extracted by liquid-liquid extraction with a MTBE/MeOH/$H_2O$ system. Specifically, 500 μL of cold MeOH was added to the cell culture dish, the contents of the dish were transferred into a 4 mL tube, 1 mL of MTBE was added, and the mixture was vortex mixed for 30 seconds. Subsequently, the mixture was vibrated for 30 min, and 250 μL of $H_2O$ was added and vortex mixed for 30 s to form a two-phase system. After equilibration for 10 min on ice, the supernatant was collected after centrifugation (14,000 rpm, 10 min, 4°C). QC samples were prepared by pooling equal aliquots of each sample. All samples were dried and stored at –80°C before liquid-chromatography tandem mass spectrometry (LC-MS/MS) analysis. Similarly, an aliquot of cells was prepared for total protein assays (Beyotime Biotechnology), and the results were used for lipid normalization.

***2.8.2 LC-MS/MS analysis.*** LC-MS/MS analysis was performed with a Shimadzu Nexera UPLC system

interfaced with an 8040 triple quadrupole mass spectrometer equipped with an ESI source. The MS instrument was operated under the following conditions: spray voltage, 4.5 kV; nebulizing gas, 3 L/min; drying gas, 15 L/min; heating gas, 10 L/min; heat block temperature, 400°C; and desolvation line temperature, 250°C. Quantification of metabolites was performed with scheduled multiple reaction monitoring (MRM) in both positive and negative modes. The MRM transitions and parameters (Table S5) were based primarily on the literature for pseudotargeted lipidomics analysis [32]. The lipids were separated on an Agilent Zorbax Eclipse Plus C18 column (2.1 × 100 mm, 1.8 μm). The column temperature was maintained at 55°C. Mobile phases A and B were ACN-$H_2O$ (60–40, v/v) and IPA-ACN (90–10, v/v), respectively, and both contained 10 mM ammonium acetate. The flow rate was 0.26 mL/min. The gradient elution was performed as follows: 0–1.5 min, 32% B; 1.5–15.5 min, 32–85% B; 15.5–18 min, 85–97% B; 18–23 min, 97–100% B; and 23–30 min, 100–32% B. The dried samples were reconstituted in 40 μL IPA and 160 μL 32% B. After centrifugation (14,000 rpm, 10 min, 4°C), 5 μL supernatant was injected into the LC-MS/MS system.

***2.8.3 Data preprocessing.*** All data were obtained by LabSolutions version 5.53 and processed by application of the following rules: 1) variables detectable in more than 80% of samples in at least one group were retained; 2) variables with a relative standard deviation > 15% in QC samples were removed; and 3) missing values were imputed with half the minimum value presented in the dataset.

### 2.9 Statistical analysis

Statistical analysis was performed in GraphPad Prism 8.0 software (GraphPad Software Inc., La Jolla, CA, USA). All experiments were repeated at least three times independently, and the results are presented as mean ± standard deviation unless otherwise specified. Independent unpaired two-tailed Student's t-test was used to evaluate differences between two groups, and multiple group comparisons were analyzed with one-way analysis of variance with Bonferroni correction. $P < 0.05$ was considered statistically significant.

## 3. RESULTS

### 3.1 Establishment of GPR35 intervention cell models

GPR35 is highly expressed in the gastrointestinal tract and is more highly expressed in colorectal cancer cells [33]. In this study, the HCT116 cell line was used to establish several GPR35 intervention models, because of the high GPR35 protein expression. First, we used lentiviral transduction to regulate GPR35 expression; consequently, both the mRNA (Figure 1A) and protein (Figure 1B) expression levels of GPR35 were significantly altered. Second, we applied the relatively exclusive ligands pamoic acid (PA) or ML194 to activate or inhibit GPR35, respectively. As shown in Figure 1C, the receptor internalization rate increased with PA treatment in a dose-dependent manner, whereas ML194 treatment at 10 μM strongly antagonized this effect. In addition, the phosphorylation of ERK1/2, which is known to be downstream of GPR35, was also increased by PA treatment or decreased by ML194 treatment (Figure 1D), although GPR35 mRNA and protein expression were unchanged (Figure 1D, E). Thus, the GPR35 intervention models were established successfully, and were considered suitable for further metabolomics and lipidomics analysis.

### 3.2 Analysis of GPR35-associated metabolites

***3.2.1 Screening of GPR35-associated metabolites through targeted metabolomics analysis.*** Targeted metabolomics analysis of GPR35 intervention cells was performed to identify metabolites differentially present between the control group and the model groups including GPR35 knock-down (KDNC vs KD), over-expression (OENC vs OE), activation (C vs PA) and inhibition (C vs ML). As shown in the volcano plots (Figure S1), the GPR35 interventions induced significant changes in the metabolic profile. A total of 75 metabolites meeting the standards of fold change > 1.5 and adjusted $P < 0.05$ were selected. As shown in the heat maps (Figure 2A–D), the metabolic characteristics significantly differed between the model groups and controls.

***3.2.2 HAA and Ura are sensitive to all GPR35 interventions.*** To obtain the metabolites overlapping among interventions, we imported all GPR35-associated metabolites in the four groups into VENNY 2.1 and generated a Venn diagram (Figure 3A). Levels of two metabolites, 3-hydroxyanthranilic acid (HAA) and uracil (Ura), significantly differed across all conditions, thus suggesting the sensitivity of these metabolites to GPR35 interventions. However, HAA and Ura decreased when GPR35 was activated or inhibited, and increased when GPR35 was knocked down or over-expressed (Figure 3B). These findings were inconsistent with the traditional concept in which opposite interventions result in opposite changes. We searched the literature and found a similar phenomenon reported in a study of the relationship between GPR35 and hypoxia-inducible factor-1α (HIF-1α) [34] or $Na^+/K^+$-ATPase [6, 7]. Specifically, HIF-1α expression is up-regulated when GPR35 is activated or inhibited, and intracellular $Ca^{2+}$ concentrations increase when GPR35 is knocked out or activated.

***3.2.3 Metabolite variation trends.*** We further analyzed the variation trends of metabolites under the different interventions and graded the metabolite levels (Table S6), on the basis of two main premises 1) GPR35 knock-down and over-expression causing opposite trends, and 2) GPR35 activation and inhibition causing opposite trends. Level 1 metabolites meeting the above two

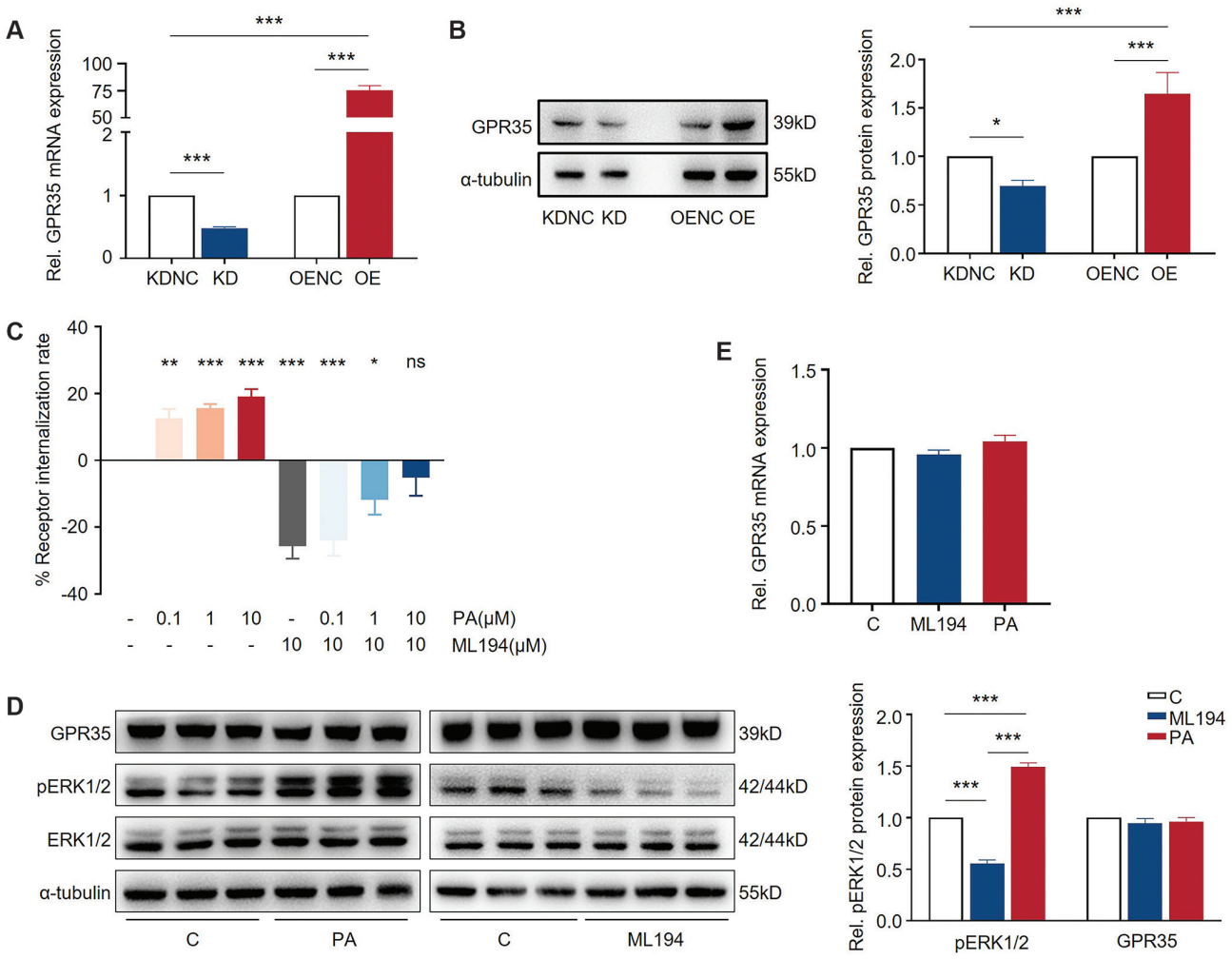


**Figure 1 | Establishment of various GPR35 intervention models.**
(A) mRNA and (B) protein levels of GPR35 post lentiviral knock-down or over-expression (n = 3). (C) GPR35 receptor internalization rate in HCT116 cells treated with PA or ML194 (n = 3). (D) GPR35 and ERK1/2 phosphorylation level in HCT116 cells treated with PA or ML194 (n = 3). (E) mRNA level of GPR35 in HCT116 cells treated with PA or ML194 (*n* = 3). **P* < 0.05, ***P* < 0.01, ****P* < 0.001. ns, Not significant; C, control; KD, knock-down; OE, over-expression; NC, negative control; PA, pamoic acid; GPR35, G protein-coupled receptor 35; ERK1/2, extracellular-regulated kinase 1/2.

premises showed the same trend in GPR35 knock-down and inhibition. Level 2 metabolites meeting the above two premises showed the same trend in GPR35 knock-down and activation. Level 3 metabolites met only one of the two premises. Level 4 metabolites met neither premise. Level 1–3 metabolites and their variation trends are shown in Figure 4. Kynurenic acid (KA) was the only level 1 metabolite: this endogenous agonist of GPR35 increased when GPR35 was inhibited or knocked down, and decreased when GPR35 was activated or over-expressed (Figure 4A). These findings suggested that GPR35 regulates KA through negative feedback, given that KA is usually considered an endogenous ligand of GPR35. Adenosine (Ado), a level 2 metabolite, decreased when GPR35 was activated or knocked down (Figure 4B). In addition, L-isoleucine, octanoic acid, and L-aspartic acid were identified as level 3 metabolites (Figure 4C, E).

***3.2.4 GPR35 interventions significantly perturb fatty acid β-oxidation.*** GPR35-associated metabolites were analyzed by compound class (e.g., fatty acids, acylcarnitines, and amino acids). As shown in Figure 5A, fatty acids and acylcarnitines were dominant among all metabolite classes. Enrichment analysis based on GPR35-associated fatty acids and acylcarnitines indicated that fatty acid β-oxidation (FAO) of very long chain fatty acids showed the greatest perturbation (Figure 5B).

## 3.3 Analysis of GPR35-associated lipids

***3.3.1 GPR35-associated lipid screening through pseudo-targeted lipidomics analysis.*** Pseudotargeted lipidomics

Acta Materia Medica

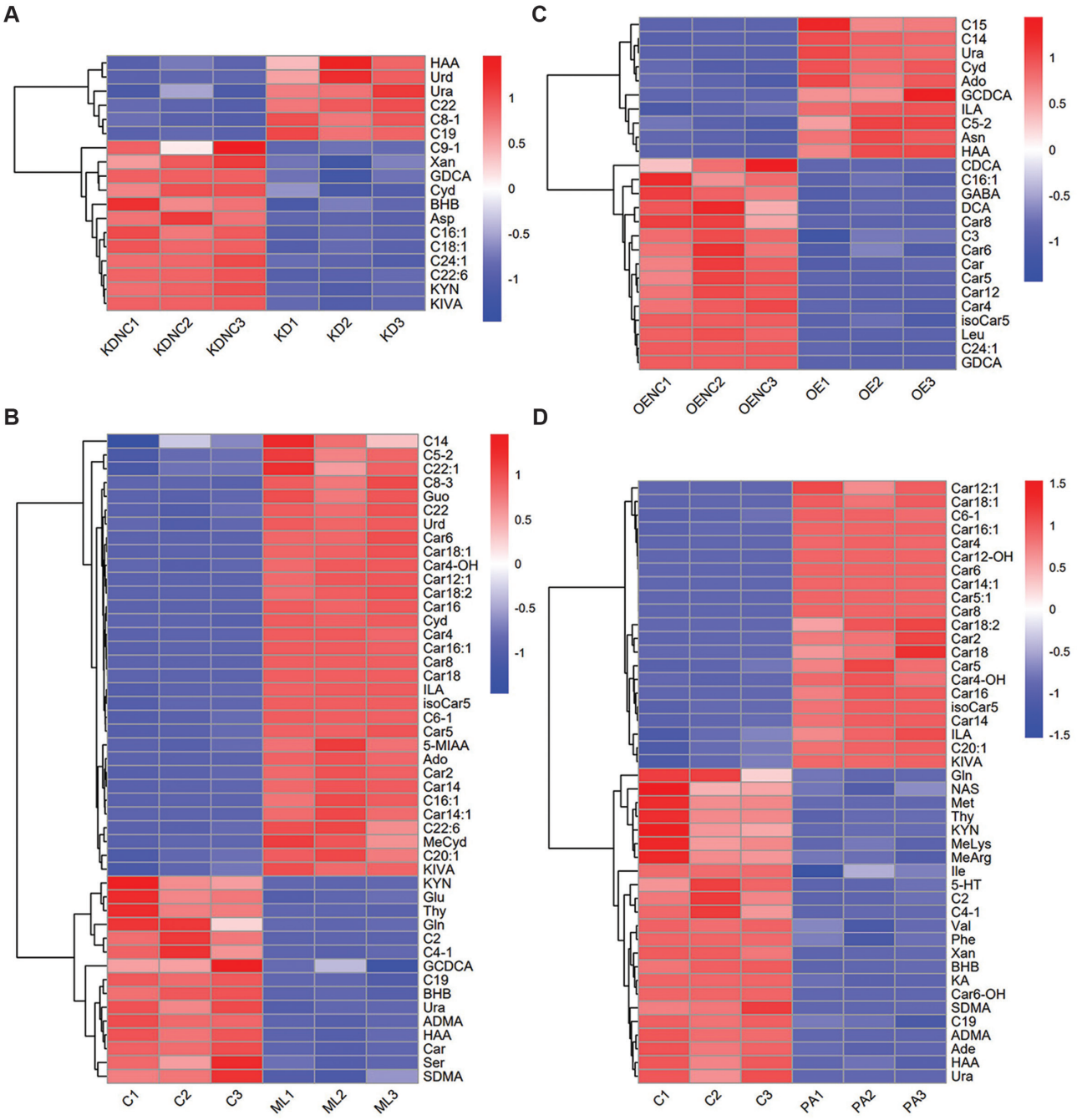


**Figure 2 | Heat maps illustrating metabolic changes induced by GPR35.**
(A) knock-down, (B) over-expression, (C) activation, and (D) inhibition. Red indicates higher and blue lower levels of metabolites. GPR35, G protein-coupled receptor 35.

analysis was performed to identify lipids differentially present across four cell models. On the basis of previous literature [32], 350 lipids were monitored in this study (**Table S5**). QC samples were included in the analytical batch for data quality evaluation. All lipids in the QC samples showed little variation, with a relative SD <15% (**Figure S2A**), and principal component analysis demonstrated that the QC samples were closely clustered (**Figure S2B, C**), thus suggesting the good stability and reproducibility of the method. GPR35-associated lipids were screened according to the same standards used in the metabolomics, and volcano plots were obtained (**Figure S3**). Consequently, 204 differentially present lipids were characterized as GPR35-associated lipids,

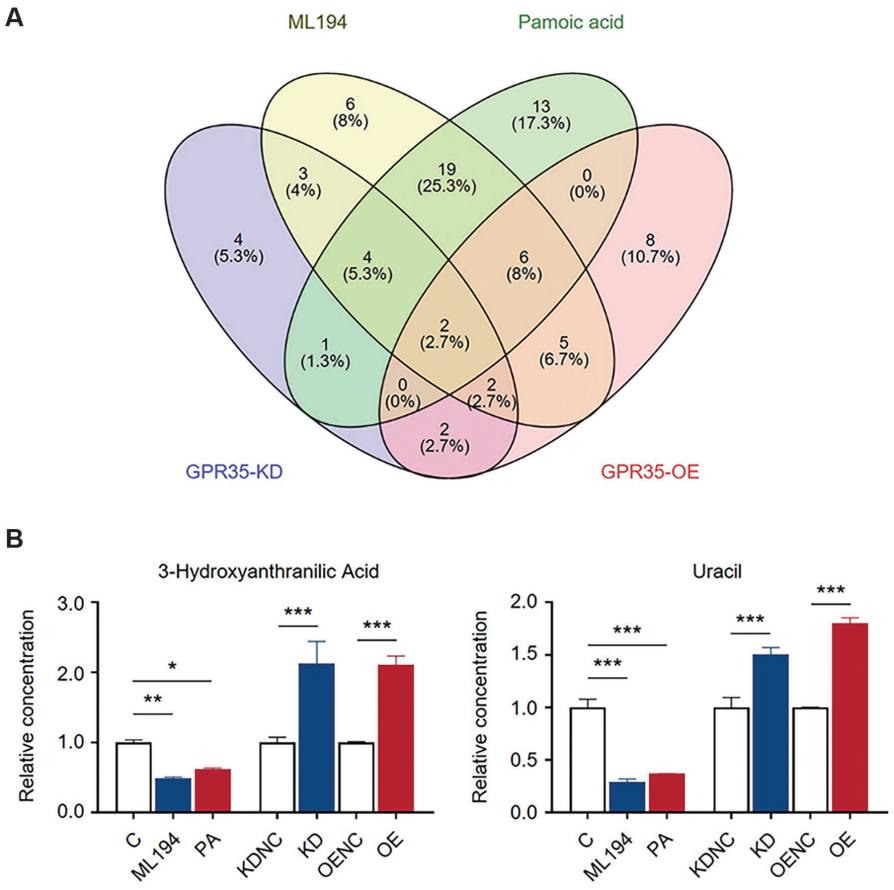


**Figure 3 | Overlapping metabolites under different GPR35 interventions.**
(A) Venn diagram showing overlapping changed metabolites induced by different GPR35 interventions. (B) Relative concentration of HAA and Ura under different GPR35 interventions compared to corresponding control groups. *$P$ < 0.05, **$P$ < 0.01, ***$P$ < 0.001. GPR35, G protein-coupled receptor 35.

thus indicating extensive changes in the lipid profile with the GPR35 interventions. The heat maps of these differentially present lipids are shown in Figure 6A–D. Similarly to the findings regarding the metabolites, lipid metabolism was significantly altered in the model groups compared with the controls. In particular, most lipids decreased with GPR35 activation (Figure 6D).

***3.3.2 No lipids showed significant changes in abundance under all interventions.*** Overlapping lipids under the different interventions were analyzed similarly to the metabolomics analyses. As shown in the Venn diagram (Figure 7), no lipids showed significant changes in abundance under all interventions. In contrast, 125 lipids showed significant changes in abundance when GPR35 was activated, in agreement with the heat map analysis, thereby suggesting that GPR35 activation caused more significant changes in lipid metabolism than GPR35 inhibition. Furthermore, 35 lipids showed changes in abundance when GPR35 was knocked down or activated; therefore, opposite interventions might not necessarily cause opposite change trends in lipid levels.

***3.3.3 Lipid variation trends.*** Similarly, we analyzed the variation trends in lipid levels by applying the same criteria described above in the metabolomics section. Level 1–4 lipids and their relative ratios are shown in Table S7. Among them, 56 lipids were identified as level 1, including primarily 20 phosphatidyl ethanolamines (PEs), 13 phosphatidylcholines, and 9 sphingomyelins. As with KA, these lipids showed increased concentrations when GPR35 was inhibited or knocked down, and decreased concentrations when GPR35 was activated or over-expressed. Eight lipids graded as level 2 showed reverse changes with intracellular $Ca^{2+}$. Another 56 lipids were classified as level 3, most of which were phosphatidylcholines. The concentrations of these lipids significantly decreased when GPR35 was activated and increased when GPR35 was inhibited, whereas no significant change was observed when the expression of GPR35 was regulated.

***3.3.4 PE metabolism is significantly perturbed by GPR35 interventions.*** We analyzed the changes according to lipid subclass by referring to the existing literature. Triglyceride (TGs) significantly decreased with GPR35

Acta Materia Medica

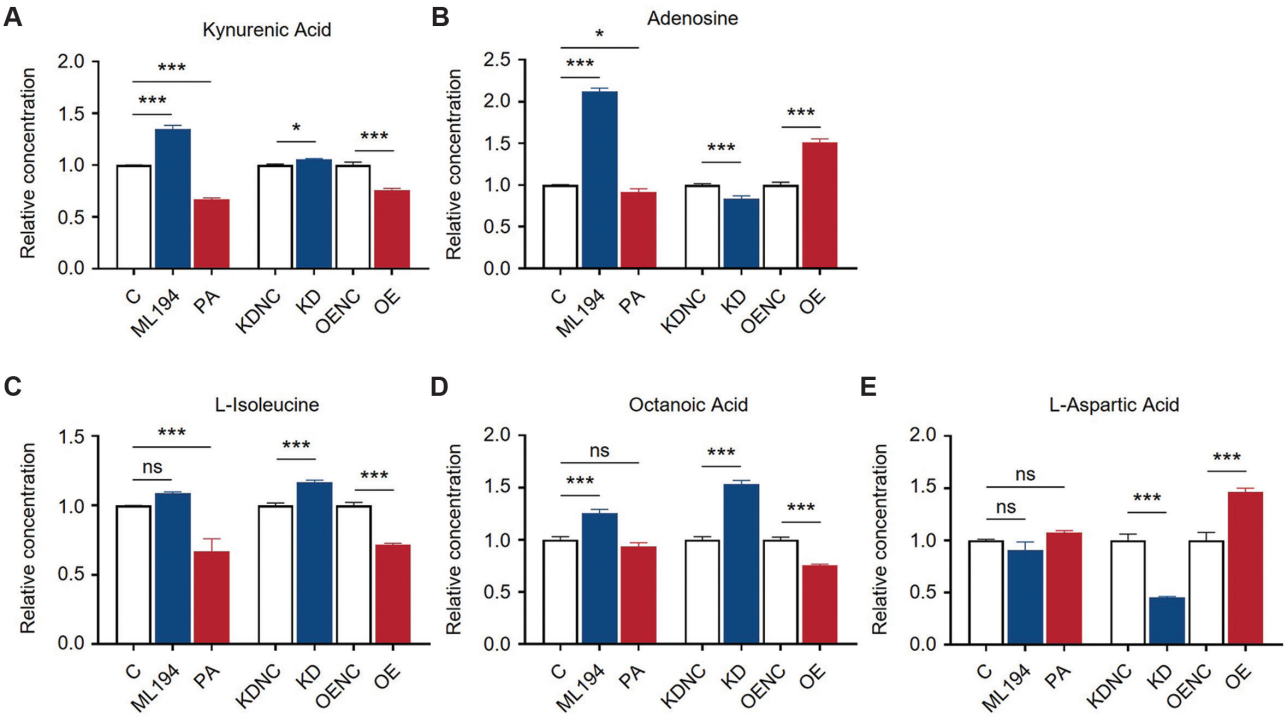


**Figure 4 | Level 1–3 metabolites and their relative concentrations under different interventions compared to corresponding controls.**

(A) Kynurenic acid (level 1), (B) adenosine (level 2), (C) L-isoleucine (level 3), (D) octanoic acid (level 3), and (E) L-aspartic acid (level 3). $*P < 0.05$, $***P < 0.001$. ns, Not significant.

knock-down and increased with GPR35 over-expression (Table S8). However, this finding must be validated by inclusion of more TGs in the analysis in the future. Moreover, PEs significantly increased with GPR35 inhibition or knock-down, and significantly decreased with GPR35 activation or over-expression (Figure 8, Table S8). Thus, PE metabolism was significantly perturbed by the GPR35 interventions.

## 4. DISCUSSION

GPR35 is closely associated with various pathophysiological conditions and has been demonstrated to be a crucial target for therapeutic interventions. However, little is known regarding the metabolic characteristics of GPR35. In some diseases, the protein levels of GPR35 have been reported to be altered; for example, GPR35 protein is up-regulated under inflammatory challenge [35] or hypoxia (such as myocardial infarction) [21], and is down-regulated in patients with UC [36]. In some cases, however, only GPR35 activity is altered; for instance, GPR35 is involved in mediating ischemic protection [12] and neutrophil recruitment [9] activated by KA or 5-Hydroxyindoleacetic acid. Therefore, we constructed four cell models with regulation of GPR35 expression or activity, to understand the related metabolic changes.

Our findings indicated that FAO was significantly perturbed by the GPR35 interventions. To date, no direct link between GPR35 and key enzymes in FAO has been reported. Ni et al. [37] have found that activated HIF-1α causes down-regulation of CPT1 in HCT116 cells, thus resulting in the accumulation of fatty acids and lipids. Moreover, HIF-1α is activated by GPR35 activation or inhibition [34]. Therefore, we hypothesized that GPR35 might affect FAO by activating HIF-1α. In contrast, GPR35 might modulate the concentrations of relevant metabolites by affecting classic FAO targets, such as peroxisome proliferator-activated receptor [38], PGC-1α [19, 39], and LXR [29, 39]. For example, activated GPR35 up-regulates PGC-1α [19], and PGC-1α in turn increases FAO to meet energy requirements [39].

Notably, we observed that PE metabolism was perturbed by the GPR35 interventions. PEs are important components of biological membranes, and have diverse roles in cellular functions such as autophagy [40], ferroptosis [41], and immune cell differentiation [42]. Dysregulation of PEs has been implicated in many metabolic diseases, such as atherosclerosis, insulin resistance, and obesity [43, 44], as well as several chronic diseases, such as Alzheimer's disease, Parkinson's disease, and nonalcoholic liver disease [44, 45]. GPR35 has also been implicated in type 2 diabetes mellitus [26, 28] and nonalcoholic liver disease [29], among others. Furthermore,

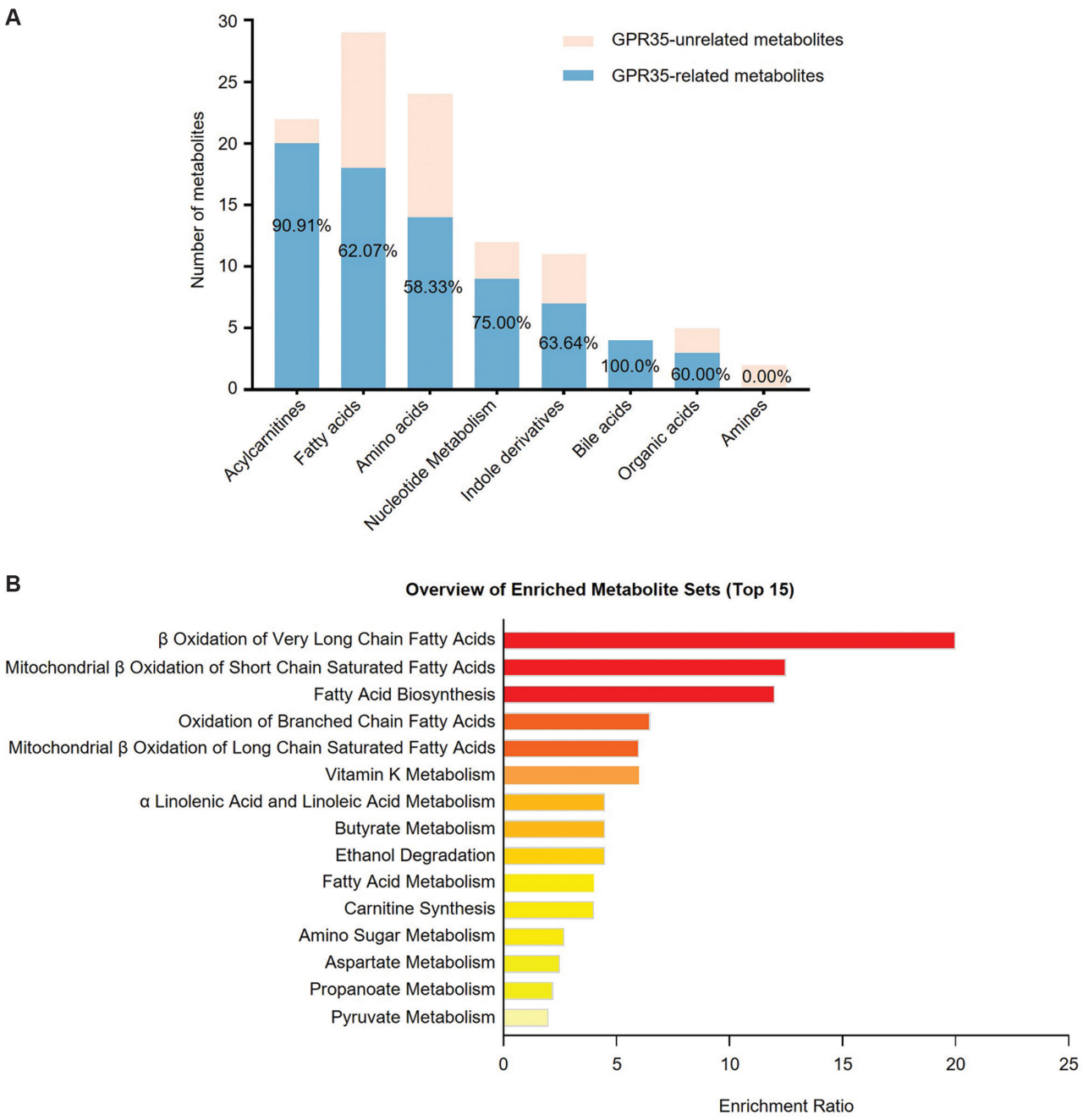


**Figure 5 | Significant disturbance of FAO by GPR35 interventions.**
(A) Distribution of GPR35-related metabolites in different metabolite classes. (B) Enrichment analysis of GPR35-related fatty acids and acylcarnitines. GPR35, G protein-coupled receptor 35.

GPR35, through up-regulation of PGC-1α, significantly affects the expression of genes associated with lipid metabolism, thermogenesis, and anti-inflammation in adipose tissue [19]. Moreover, activation of GPR35 inhibits lipid accumulation through LXR inhibition in hepatocyte [20, 29]. We speculate that these functions of GPR35 might be involved in the regulation of lipid metabolism, particularly that of PE.

Beyond FAO and PE metabolism, we identified specific metabolites sensitive to GPR35 interventions. HAA and Ura decreased with interventions altering GPR35 activity and increased with interventions altering GPR35 expression. These findings were consistent with the changes in HIF-1α [34] or $Na^+/K^+$-ATPase reported in prior studies [6, 7]. Other metabolites, such as KA and Ado, exhibited opposite changes following GPR35 knock-down and

Acta Materia Medica

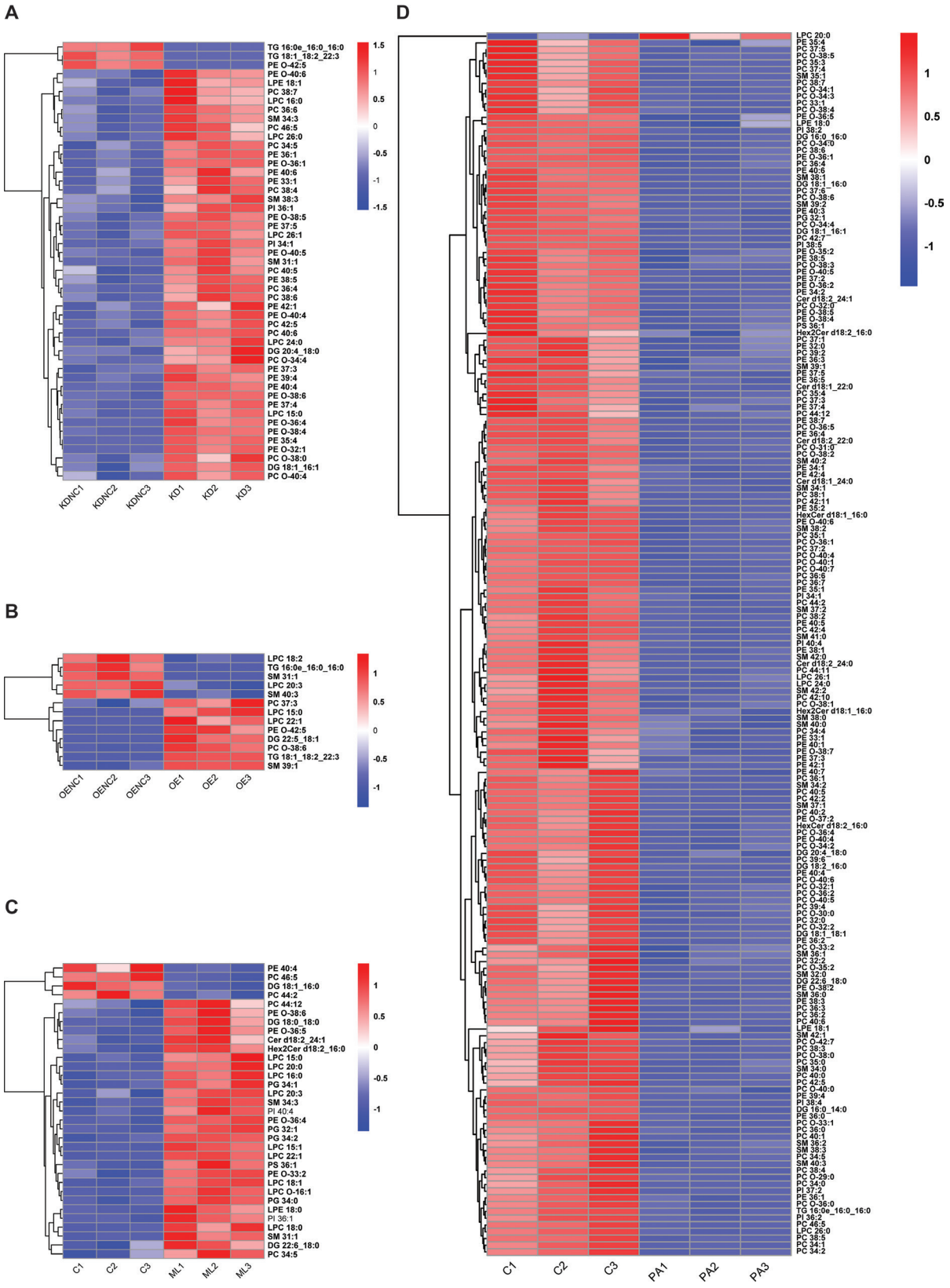


**Figure 6 | Heat maps displaying significant changes in lipid profile induced by GPR35.**
(A) Knock-down, (B) over-expression, (C) activation, and (D) inhibition. GPR35, G protein-coupled receptor 35.

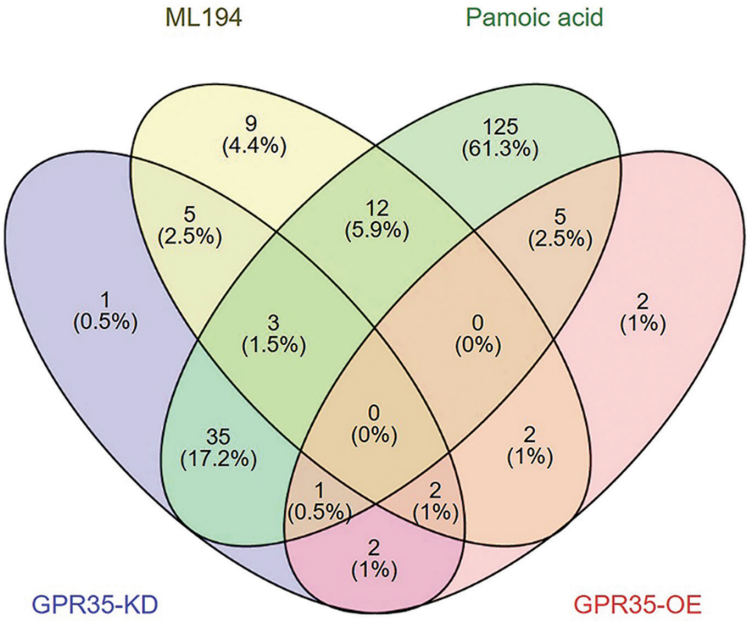


**Figure 7 | Venn diagram illustrating overlapping lipids under various GPR35 interventions.**
GPR35, G protein-coupled receptor 35.

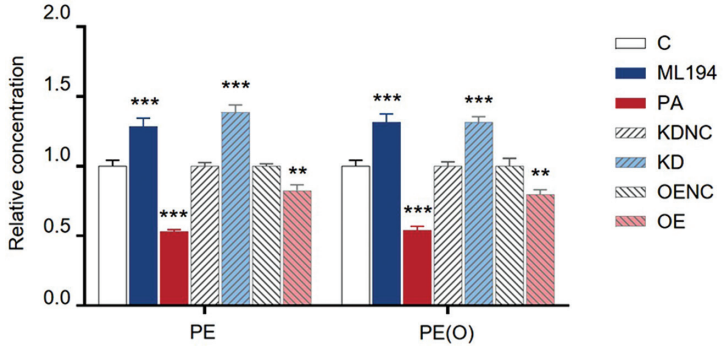


**Figure 8 | Significant disturbance of PE metabolism by GPR35 interventions.**
$^{**}P < 0.01$, $^{***}P < 0.001$. PE(O), alkyl or alkenyl substituent PE; PE, phosphatidylethanolamines; GPR35, G protein-coupled receptor 35.

over-expression, as well as opposite changes following GPR35 activation and inhibition. The KA-GPR35 axis is involved in various physiological and pathological processes, such as inflammation, analgesia, and cardiovascular system diseases [4, 12, 17]. Ado, similarly to GPR35, is significantly up-regulated under stress states, such as inflammation, ischemia, and hypoxia [46].

This study has several limitations, and our findings require further exploration. For example, experiments are necessary to confirm the links between GPR35 and FAO or PE metabolism. Future investigations may include 1) measurement of all metabolites involved in FAO or PE metabolism in the four cell models to confirm the relationship between GPR35 intervention and these two pathways; 2) exploration of the changes in expression or activity of key enzymes/genes in FAO or PE metabolism under GPR35 interventions; and 3) further validation of through the regulation of related enzymes/genes under GPR35 interventions. In addition, our experiments were performed solely in a cell model, which cannot fully represent the metabolic regulation of GPR35 in vivo; consequently, animal experiments are necessary to confirm our findings.

## 5. CONCLUSIONS

GPR35 has widespread pathophysiological associations with many diseases and has gained increasing attention as a promising treatment target. However, the study of GPR35 remains in its infancy. To our knowledge, this study is the first to report the metabolic characteristics of GPR35, according to targeted metabolomics and

pseudotargeted lipidomics. Many metabolites and lipids showed marked changes in abundance under the different GPR35 interventions, among which FAO and PE metabolism were significantly perturbed. Although further experiments are required to validate our findings, our data may promote understanding of the metabolic characteristics of GPR35.

## ACKNOWLEDGEMENTS

This study was supported by the NSFC (No. 82073812, 82104117, and 82273896), Natural Science Foundation of Jiangsu Province (No. BK20210427), Double First-Class Project of China Pharmaceutical University (CPUQNJC22_02), Program for Jiangsu province Innovative Research Team, and a project funded by the Priority Academic Program Development of Jiangsu Higher Education Institutions (PAPD).

## CONFLICTS OF INTEREST

The authors declare no conflicts of interest.

## CREDIT AUTHOR STATEMENT

Q. Z.: Formal analysis, Investigation, Writing—Original Draft Preparation. X. Z.: Writing—Reviewing and Editing, Visualization. S. Q.: Methodology. Q. X.: Visualization. Y. T.: Methodology, Resources. Z. Z.: Resources, Funding Acquisition. P. Z.: Conceptualization, Supervision, Writing—Reviewing and Editing, Funding Acquisition. F. X.: Conceptualization, Supervision, Writing—Reviewing and Editing, Funding Acquisition.

## REFERENCES

[1] Santos R, Ursu O, Gaulton A, Bento AP, Donadi RS, Bologa CG, et al.: A Comprehensive Map of Molecular Drug Targets. *Nature Reviews Drug Discovery* 2017, 16(1):19–34.

[2] O'Dowd BF, Nguyen T, Marchese A, Cheng R, Lynch KR, Heng HH, et al.: Discovery of Three Novel G-Protein-Coupled Receptor Genes. *Genomics* 1998, 47(2):310–313.

[3] Okumura S, Baba H, Kumada T, Nanmoku K, Nakajima H, Nakane Y, et al.: Cloning of a G-Protein-Coupled Receptor that Shows an Activity to Transform NIH3T3 Cells and is Expressed in Gastric Cancer Cells. *Cancer Science* 2004, 95(2):131–135.

[4] Quon T, Lin LC, Ganguly A, Tobin AB, Milligan G: Therapeutic Opportunities and Challenges in Targeting the Orphan G Protein-Coupled Receptor GPR35. *ACS Pharmacology and Translational Science* 2020, 3(5):801–812.

[5] Farooq SM, Hou Y, Li H, O'Meara M, Wang Y, Li C, et al.: Disruption of GPR35 Exacerbates Dextran Sulfate Sodium-Induced Colitis in Mice. *Digestive Diseases and Sciences* 2018, 63(11):2910–2922.

[6] Pagano E, Elias JE, Schneditz G, Saveljeva S, Holland LM, Borrelli F, et al.: Activation of the GPR35 Pathway Drives Angiogenesis in the Tumour Microenvironment. *Gut* 2022, 71(3):509–520.

[7] Schneditz G, Elias JE, Pagano E, Zaeem Cader M, Saveljeva S, Long K, et al.: GPR35 Promotes Glycolysis, Proliferation, and Oncogenic Signaling by Engaging with the Sodium Potassium Pump. *Science Signaling* 2019, 12(562):eaau9048.

[8] Fallarini S, Magliulo L, Paoletti T, de Lalla C, Lombardi G: Expression of functional GPR35 in Human iNKT Cells. *Biochemical and Biophysical Research Communications* 2010, 398(3):420–425.

[9] De Giovanni M, Tam H, Valet C, Xu Y, Looney MR, Cyster JG: GPR35 Promotes Neutrophil Recruitment in Response to Serotonin Metabolite 5-HIAA. *Cell* 2022, 185(5):815–830.e19.

[10] Barth MC, Ahluwalia N, Anderson TJ, Hardy GJ, Sinha S, Alvarez-Cardona JA, et al.: Kynurenic Acid Triggers Firm Arrest of Leukocytes to Vascular Endothelium Under Flow Conditions. *The Journal of Biological Chemistry* 2009, 284(29):19189–19795.

[11] Min KD, Asakura M, Liao Y, Nakamaru K, Okazaki H, Takahashi T, et al.: Identification of Genes Related to Heart Failure Using Global Gene Expression Profiling of Human Failing Myocardium. *Biochemical and Biophysical Research Communications* 2010, 393(1):55–60.

[12] Wyant GA, Yu W, Doulamis IP, Nomoto RS, Saeed MY, Duignan T, et al.: Mitochondrial Remodeling and Ischemic Protection by G Protein-Coupled Receptor 35 Agonists. *Science* 2022, 377(6606):621–629.

[13] Divorty N, Milligan G, Graham D, Nicklin SA: The Orphan Receptor GPR35 Contributes to Angiotensin II-Induced Hypertension and Cardiac Dysfunction in Mice. *American Journal of Hypertension* 2018, 31(9):1049–1058.

[14] Zhao P, Sharir H, Kapur A, Cowan A, Geller EB, Adler MW, et al.: Targeting of the Orphan Receptor GPR35 by Pamoic Acid: A Potent Activator of Extracellular Signal-Regulated Kinase and β-Arrestin2 with Antinociceptive Activity. *Molecular Pharmacology* 2010, 78(4):560–568.

[15] Divorty N, Mackenzie AE, Nicklin SA, Milligan G: G Protein-Coupled Receptor 35: An Emerging Target in Inflammatory and Cardiovascular Disease. *Frontiers in Pharmacology* 2015, 6:41.

[16] Ohshiro H, Tonai-Kachi H, Ichikawa K: GPR35 is a Functional Receptor in Rat Dorsal Root Ganglion Neurons. *Biochemical and Biophysical Research Communications* 2008, 365(2):344–348.

[17] Sun T, Xie R, He H, Xie Q, Zhao X, Kang G, et al.: Kynurenic Acid Ameliorates NLRP3 Inflammasome Activation by Blocking Calcium Mobilization Via GPR35. *Frontiers in Immunology* 2022, 13:1019365.

[18] Tsukahara T, Hamouda N, Utsumi D, Matsumoto K, Amagase K, Kato S: G Protein-Coupled Receptor 35 Contributes to Mucosal Repair in Mice Via Migration of Colonic Epithelial Cells. *Pharmacological Research* 2017, 123:27–39.

[19] Agudelo LZ, Ferreira DMS, Cervenka I, Bryzgalova G, Dadvar S, Jannig PR, et al.: Kynurenic Acid and Gpr35 Regulate Adipose Tissue Energy Homeostasis and Inflammation. *Cell Metabolism* 2018, 27(2):378–392.e5.

[20] Nam SY, Park SJ, Im DS: Protective Effect of Lodoxamide on Hepatic Steatosis Through GPR35. *Cell Signal* 2019, 53:190–200.

[21] Ronkainen VP, Tuomainen T, Huusko J, Laidinen S, Malinen M, Palvimo JJ, et al.: Hypoxia-Inducible Factor 1-Induced G Protein-Coupled Receptor 35 Expression is an Early Marker of Progressive Cardiac Remodelling. *Cardiovascular Research* 2014, 101(1):69–77.

[22] McCallum JE, Mackenzie AE, Divorty N, Clarke C, Delles C, Milligan G, et al.: G-Protein-Coupled Receptor 35 Mediates Human Saphenous Vein Vascular Smooth

Muscle Cell Migration and Endothelial Cell Proliferation. *Journal of Vascular Research* 2015, 52(6):383–395.

[23] Jenkins L, Brea J, Smith NJ, Hudson BD, Reilly G, Bryant NJ, et al.: Identification Of Novel Species-Selective Agonists of the G-Protein-Coupled Receptor GPR35 that Promote Recruitment of β-Arrestin-2 and Activate Gα13. *The Biochemical Journal* 2010, 432(3):451–459.

[24] Neetoo-Isseljee Z, MacKenzie AE, Southern C, Jerman J, McIver EG, Harries N, et al.: High-Throughput Identification and Characterization of Novel, Species-Selective GPR35 Agonists. *The Journal of Pharmacology and Experimental Therapeutics* 2013, 344(3):568–578.

[25] Kwon Y, Mehta S, Clark M, Walters G, Zhong Y, Lee HN, et al.: Non-Canonical β-Adrenergic Activation of ERK at Endosomes. *Nature* 2022, 611(7934):173–179.

[26] Tan JK, McKenzie C, Marino E, Macia L, Mackay CR: Metabolite-Sensing G Protein-Coupled Receptors-Facilitators of Diet-Related Immune Regulation. *Annual Review of Immunology* 2017, 35:371–402.

[27] Dadvar S, Ferreira DMS, Cervenka I, Ruas JL: The Weight of Nutrients: Kynurenine Metabolites in Obesity and Exercise. *Journal of Internal Medicine* 2018, 284(5):519–533.

[28] Jung TW, Park J, Sun JL, Ahn SH, Abd El-Aty AM, Hacimuftuoglu A, et al.: Administration of Kynurenic Acid Reduces Hyperlipidemia-Induced Inflammation and Insulin Resistance in Skeletal Muscle and Adipocytes. *Molecular and Cellular Endocrinology* 2020, 518:110928.

[29] Lin LC, Quon T, Engberg S, Mackenzie AE, Tobin AB, Milligan G: G protein-coupled Receptor GPR35 Suppresses Lipid Accumulation in Hepatocytes. *ACS Pharmacology AND Translational Science* 2021, 4(6):1835–1848.

[30] Jiang R, Jiao Y, Zhang P, Liu Y, Wang X, Huang Y, et al.: Twin Derivatization Strategy for High-Coverage Quantification of Free Fatty Acids by Liquid Chromatography-Tandem Mass Spectrometry. *Analytical Chemistry* 2017, 89(22):12223–12230.

[31] Qin S, Gao M, Zhang Q, Xiao Q, Fu J, Tian Y, et al.: High-Coverage Strategy for Multi-Subcellular Metabolome Analysis Using Dansyl-Labeling-Based LC-MS/MS. *Analytical Chemistry* 2023, 95:10034–10043.

[32] Xuan Q, Hu C, Yu D, Wang L, Zhou Y, Zhao X, et al.: Development of a High Coverage Pseudotargeted Lipidomics Method Based on Ultra-High Performance Liquid Chromatography-Mass Spectrometry. *Analytical Chemistry* 2018, 90(12):7608–7616.

[33] Yao H, Lv Y, Bai X, Yu Z, Liu X: Prognostic Value of CXCL17 and CXCR8 Expression in Patients with Colon Cancer. *Oncology Letters* 2020, 20(3):2711–2720.

[34] Hu HH, Deng H, Ling S, Sun H, Kenakin T, Liang X, et al.: Chemical Genomic Analysis of GPR35 Signaling. *Integrative Biology (Camb)* 2017, 9(5):451–463.

[35] Yang Y, Lu JY, Wu X, Summer S, Whoriskey J, Saris C, et al.: G-Protein-Coupled Receptor 35 is a Target of the Asthma Drugs Cromolyn Disodium and Nedocromil Sodium. *Pharmacology* 2010, 86(1):1–5.

[36] Kaya B, Donas C, Wuggenig P, Diaz OE, Morales RA, Melhem H, et al.: Lysophosphatidic Acid-Mediated GPR35 Signaling in CX3CR1(+) Macrophages Regulates Intestinal Homeostasis. *Cell Reports* 2020, 32(5): 107979.

[37] Ni T, He Z, Dai Y, Yao J, Guo Q, Wei L: Oroxylin A Suppresses the Development and Growth of Colorectal Cancer Through Reprogram of HIF1α-Modulated Fatty Acid Metabolism. *Cell Death and Disease* 2017, 8(6):e2865.

[38] Nakamura MT, Yudell BE, Loor JJ: Regulation of Energy Metabolism by Long-Chain Fatty Acids. *Progress in Lipid Research* 2014, 53:124–144.

[39] Zhang Y, Castellani LW, Sinal CJ, Gonzalez FJ, Edwards PA: Peroxisome Proliferator-Activated Receptor-Gamma Coactivator 1alpha (PGC-1alpha) Regulates Triglyceride Metabolism by Activation of the Nuclear receptor FXR. *Genes and Development* 2004, 18(2):157–169.

[40] Rockenfeller P, Koska M, Pietrocola F, Minois N, Knittelfelder O, Sica V, et al.: Phosphatidylethanolamine Positively Regulates Autophagy and Longevity. *Cell Death and Differentiation* 2015, 22(3):499–508.

[41] Zou Y, Palte MJ, Deik AA, Li H, Eaton JK, Wang W, et al.: A GPX4-Dependent Cancer Cell State Underlies the Clear-Cell Morphology and Confers Sensitivity to Ferroptosis. *Nature Communications* 2019, 10(1):1617.

[42] Fu G, Guy CS, Chapman NM, Palacios G, Wei J, Zhou P, et al.: Metabolic Control of T(FH) Cells and Humoral Immunity by Phosphatidylethanolamine. *Nature* 2021, 595(7869):724–729.

[43] van der Veen JN, Kennelly JP, Wan S, Vance JE, Vance DE, Jacobs RL: The Critical Role of Phosphatidylcholine and Phosphatidylethanolamine Metabolism in Health and Disease. *Biochimica et Biophysica Acta Biomembranes* 2017, 1859(9 Pt B):1558–1572.

[44] Pohl EE, Jovanovic O: The Role of Phosphatidylethanolamine Adducts in Modification of the Activity of Membrane Proteins under Oxidative Stress. *Molecules* 2019, 24(24):4545.

[45] Calzada E, Onguka O, Claypool SM: Phosphatidylethanolamine Metabolism in Health and Disease. *International Review of Cell and Molecular Biology* 2016, 321:29–88.

[46] Linden J: Molecular Approach to Adenosine Receptors: Receptor-Mediated Mechanisms of Tissue Protection. *Annual Review of Pharmacology and Toxicology* 2001, 41:775–787.